Afterglow mode and the new Micro Pulsed Beam mode applied to an ECR Ion Source

Laurent Maunoury, Lamri Adoui, Jean-Pierre Grandin, Bernd Huber, Emily Lamour, P. Lehérissier, Fabien Noury, J.Y. Pacquet, Christophe Prigent, Jean-Pierre Rozet, et al.

Afterglow mode and the new Micro Pulsed Beam mode applied to an ECR Ion Source[a]

L. Maunoury[1)], L. Adoui[1)], J.P. Grandin[1)], B.A. Huber[1)], E. Lamour[2)], P. Leherissier[3)], F. Noury[1)], J.Y. Pacquet[3)], C. Prigent[2)], J.P. Rozet[2)] and D. Vernhet[2)]

1) CIRIL, Bd Henri Becquerel, BP 5133, F-14070 Caen cedex 05, France

2) INSP Paris 6, Campus Boucicaut, 140 rue de Lourmel, F-75015 Paris, France

3) GANIL, bd H. Becquerel BP 55027, F-14076 Caen cedex 05, France

Abstract

An increasing number of experiments in the field of low energy ion physics (< 25 keV/charge) requires pulsed beams of highly charged ions. Whereas for high-intensity beams (> µA) a pulsed beam chopper, installed downstream to the analyzing dipole, is used. For low-intensity beams (< 100 nA) the ion intensity delivered during the pulse may be increased by operating the ECR discharge in the afterglow mode [1]. This method gives satisfactory results (ie average current during the beam pulse is higher than the current in the CW mode) for high charge state ions. In this paper, we report on results of the afterglow mode for beams of $^{22}Ne^{q+}$, $^{36}Ar^{q+}$ and $^{84}Kr^{q+}$ ions. Furthermore, a new promising "Micro Pulsed Beam" mode will be described with encouraging preliminary results for $^{84}Kr^{27+}$ and $^{36}Ar^{17+}$ ions.

PACS N°: 07.77.Ka, 29.25.Ni, 52.50-Sw, 52.25.Jm

Keywords: plasma ion sources, electron cyclotron resonance, afterglow discharge, particle beam bunching

---

[a] **Contributed paper, published as part of the Proceedings of the 12th International Conference on Ion Sources, Jeju, Korea, August 2007**

I. Introduction

The ‘afterglow’ mode has been applied to an ECR ion source (ECRIS) more than one decade ago[1,2]. This technique was initially developed for the production of an intense pulsed beam of Pb^{n+} ions for the CERN accelerator. There are two methods to create an afterglow discharge: either the RF power supply sustaining the discharge or the magnetic field at the extraction side of the ion source are pulsed [3]. At the end of the RF pulse or the magnetic field pulse, an electron deconfinement (electrostatic or magnetic) occurs and the multiply charged ions follow the electrons, thus yielding a high current peak of extracted ions. This method has been studied with however limited values of n for Ar^{n+} [1,3], Pb^{n+} [1,4,5], Bi^{n+} [1] and O^{n+} ions [1,4]. There exist also a systematic study for the Xe^{n+} case under different RF pulse conditions [6]. So far no references for optimized $Ne^{9+, 10+}$, Ar^{17+}, Kr^{n+} beams exist. Usually, the RF pulse width is within the range of tens of ms for obtaining a current pulse characterized by a rising time of a hundred of μs and by a long tail of roughly a few ms. In the following parts, we will present the new beam characteristics as well as a new pulsed mode, called Micro Pulsed Beam (MPB), which yields high current peak intensities for $^{36}Ar^{17+}$ and $^{84}Kr^{27+}$ ions.

II . Experimental set-up for the afterglow mode

The ECRIS used in these studies was the SUPERSHyPIE ion source which has been described in detail in the reference [7]. The RF power supply provides a microwave at 14.5 GHz frequency with a maximum power of 1.1 kW during the pulse. The repetition rate is fixed at 10Hz for all the measurements and the rise and fall time of the pulse generator (Tektronix AFG3021) is 18 ns. The time required to obtain the full RF power is 5 μs. The current set for the magnetic coils of the ECRIS is optimized in order to get the best possible plasma confinement (1.2 T at the injection side and 1 T at the extraction side). The ion bunch current is measured with a Faraday cup located at the focal plane of the analyzing dipole. The

Faraday cup is connected to ground via a 100 kΩ resistor across which the voltage drop is read out with an oscilloscope (Tektronix TDS1012). For all experiments O_2 was used as support gas. The extraction voltage was chosen to be in the 15 and 18 kV range, resulting in a transport efficiency of about 9%.

III. Experimental results

Each time the afterglow mode was optimized with the aim to maximize the current in the afterglow peak by minimizing the current during the RF pulse. The source was tuned to obtain a charge state distribution with a maximum at very high charge states. The main parameters for tuning the source were the following: the flux of the main gas, the flux of the support gas, the bias tube voltage and the RF pulse width. All the other parameters of the ion source were kept fixed.

III.a ^{22}Ne results

For the charge states 9+ and 10+ (see Fig. 1) the source delivers a regular afterglow pulse (occurring without delay just after the end of the RF pulse) with a fast and strong increase of the extracted ion current (rise time of 600 μs with a long tail of several ms). In Table, the current ratio between the afterglow mode and the CW (Continuous Wave) mode is reported. These ratios are 7.9 and 10.2 for charge states 9+ and 10+, respectively. Fig. 2 shows the evolution of the current and the FWHM (Full Width at Half Maximum) of the afterglow bunch as a function of the RF pulse width for the case $^{22}Ne^{10+}$. The FWHM follows a plateau around the value of 1.1 ms whereas the current has a maximum for an RF pulse width of 20 ms.

III.b ^{36,40}Ar results

Fig. 3 is an oscilloscope display of the afterglow peaks obtained for the Ar^{q+} cases. The afterglow mode gives an increase in the beam intensity for the charge states between 14+

and 16+ (factor 7.6 and 10 compared to the CW mode), but surprisingly it doesn't give any significant improvement for the charge state 17+. Only a factor of 1.33 is obtained, although many parameters have been optimized. The question is raised whether this might be due to the fact that the ionization energy for the production of Ar^{17+} is 3947 eV compared to the energy of 939 eV which is necessary for creating Ar^{16+}.

III.c ^{84}Kr results

In the case of $^{84}Kr^{q+}$ beams (see Fig. 4 and Table) the gain factors are generally lower than for the Ne and Ar cases. In particular, for high charge states as $^{84}Kr^{q+}$ (q = 25 and 27) the gain factor becomes smaller than 1 (see table 1). Fig. 5 shows the evolution of the FWHM of the afterglow peak and the rise time of the ion bunch as a function of the charge state. Both curves decrease with increasing charge state and reach again a plateau with a value of 1.3 ms for FWHM and 610 μs for the rise time. The latter value is comparable with those measured for Ne (553 μs) and Ar (610 μs). This result seems to prove that the production of high charge state ions (including electron heating, ionization and multiply charged ion diffusion towards the extraction zone) are similar for charge states 10+, 16+ and 23+ for Ne, Ar and Kr ions, respectively. As the energy and density of the electron population is almost the same for all the cases above (1.1 kW of power in the RF pulse and a RF frequency of 14.5 GHz), only the difference in the electron-impact ionization cross-section can explain the peak current differences and therefore the differences in the measured ratios of the $I_{Afterglow}$ over I_{CW}.

III.d Preglow mode

Sortais and his collaborators have reported in reference [5] on a new pulsed mode called 'Preglow'. This phenomenon has been observed in two different ECR sources. It is characterized by a fast peak occurring just at the beginning of the RF pulse. The explanation is based on a pumping effect and a fast ionization process [5]. We have observed the same behaviour for a higher charge state of the ion ($^{84}Kr^{27+}$; see Fig. 6). In the present experiment,

the RF pulse width was 50 ms instead of 10 ms as used in the case of reference [5]. It turns out that the Preglow peak shows a double structure: a very sharp peak (FWHM of 1.2 ms) with a high intensity (290 nA) and a second wider peak (FWHM around 12 ms) but with a lower intensity (150 nA). The shape is also different from a typical afterglow peak as no tail is observed.

IV Micro Pulsed Beam mode

As mentioned above, for the $^{36}Ar^{17+}$ beam the normal afterglow mode was not efficient. However, we discovered that an important improvement can be obtained when we operate the discharge in a new regime, namely when shortening RF pulse of around 1ms or less is used. For $^{36}Ar^{17+}$ a pulsed beam of 0.6 μA has been measured with an RF pulse width of 700 μs which corresponds to a gain factor of 20 compared to the CW mode. A similar phenomenon has been observed for the $^{84}Kr^{27+}$ pulsed beam with a current of 12 μA and a RF pulse width of 1000 μs yielding a gain factor of 29 compared to the CW mode. We succeeded to measure also an $^{84}Kr^{29+}$ pulsed beam with a RF pulse width of 400 μs giving a current of 70 nA, it hasn't been produced in CW mode. We call this new mode Micro Pulsed Beam (MPB). In Fig. 7, the pictures of the ion bunch recorded with the oscilloscope are displayed. To confirm the Q/M of the ions, they have been sent through the ARIBE L4 beam line [7] which is a magnetic beam line characterized by a specific value of Bρ (magnetic rigidity). In both cases, a pulsed beam has been measured with an intensity corresponding to the transmission of the beam line. Hence the intensities and the Q/M of the pulsed beams were well established. As it can be seen in the Fig. 7, the ion bunch has approximately a symmetric shape with a delay between the end of the RF pulse and the beginning of ion bunch. This delay may correspond to the diffusion of multiply charged ions from the production zone to the extraction location.

Fig. 8 shows the evolution of the current and the FWHM of the ion bunch as a function of the RF pulse width. The delay between the RF pulse and the ion bunch is also displayed. For the current, we observe an optimum for an RF pulse width of 800 μs. Concerning the FWHM, it increases from a value of 100 μs for an RF pulse of 200 μs until it reaches a plateau of 440 μs. The delay is measured to be of the order of 600 μs.

Fig. 9 shows a summary of the present results. It is the ratio of the current in the afterglow mode over the current measured in the CW mode (gain factor). For Ne and Ar (with the exception of Ar^{17+}), the afterglow mode gives encouraging results. Relating to Kr, the results are less successful: the gain factors are relatively low (<3) and for the higher charge states they are even less than 1. However, when applying the MPB mode, the values increase far above the values obtained with the normal afterglow mode.

When applying the MPB mode, it turned out that the ratio of the flux of the support gas over the flux of the main gas is a sensitive parameter. It should be of the order of 20. Furthermore, the power supply of the bias tube has to deliver a high electronic current (> 5mA). The observed phenomena require that a very fast ionization process is involved which can not be explained by the well established step by step ionization process in an ECR source. This means also that the electron population in terms of energy and density should reach their maxima very fast, on a time scale of < 100 μs. According to reference [8], in this time range, the life time of the hot electron population is long enough (around 5 ms) and can explain the creation of high charge state ions.

The presented method is a new way of producing high current pulsed beams. However, in order to better operate this discharge mode and to clarify the underlying processes, more studies are needed. In particular, the following questions await an answer: How does the phenomenon depend on the RF power (>1.1 kW) or on the RF frequency?

Does this process work also with other species as C^{6+} (hadrontherapy), Xe^{q+}, Pb^{q+} (CERN) etc…? What is the influence of the support gas type? What is the influence of the bias tube (in the present case the voltage was fixed at 2 kV)? Does it still work when the repetition rate increases allowing in this way the raise of the average current? Much work is needed to examine this phenomenon from every angle.

References

[1]P. Sortais et al., Rev. Sci. Instrum., **63** (4), 2801 (1992)

[2]R. Geller, *Electron Cyclotron Resonnance ion Sources and ECR Plasmas*, IOP, Bristol (1996)

[3]L. Müller et al., Rev. Sci. Instrum., **73** (3), 1140 (2002)

[4]C.E. Hill et al., Rev. Sci. Instrum., **73** (2), 564 (2002)

[5]P. Sortais et al., Rev. Sci. Instrum., **75** (5), 1610 (2004)

[6]K. Tinschert et al., Rev. Sci. Instrum., **75** (5), 1407 (2004)

[7]L. Maunoury et al., Rev. Sci. Instrum., **73** (2), 561 (2002)

[8]C. Barue, Phd-Thesis, Paris 6 University (1992)

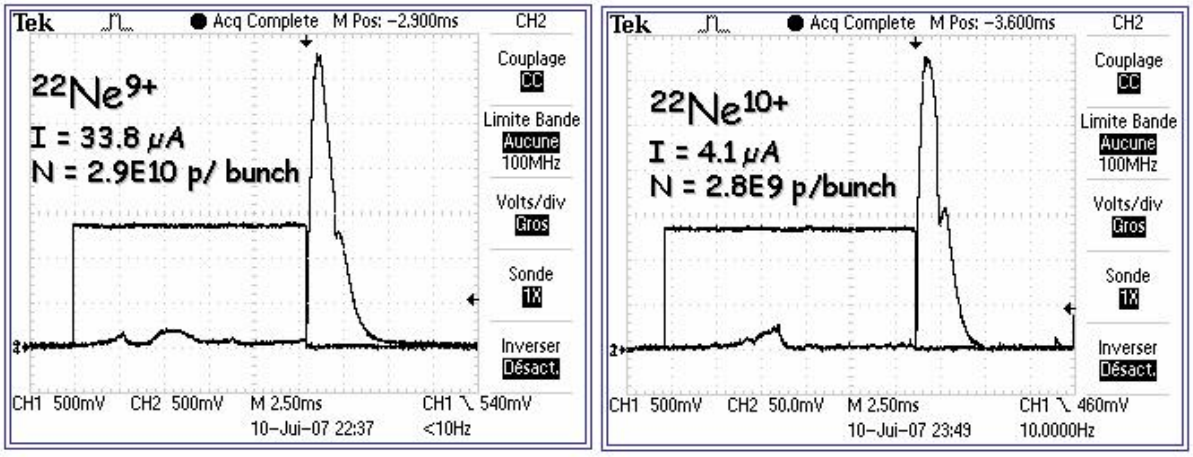

Figure 1

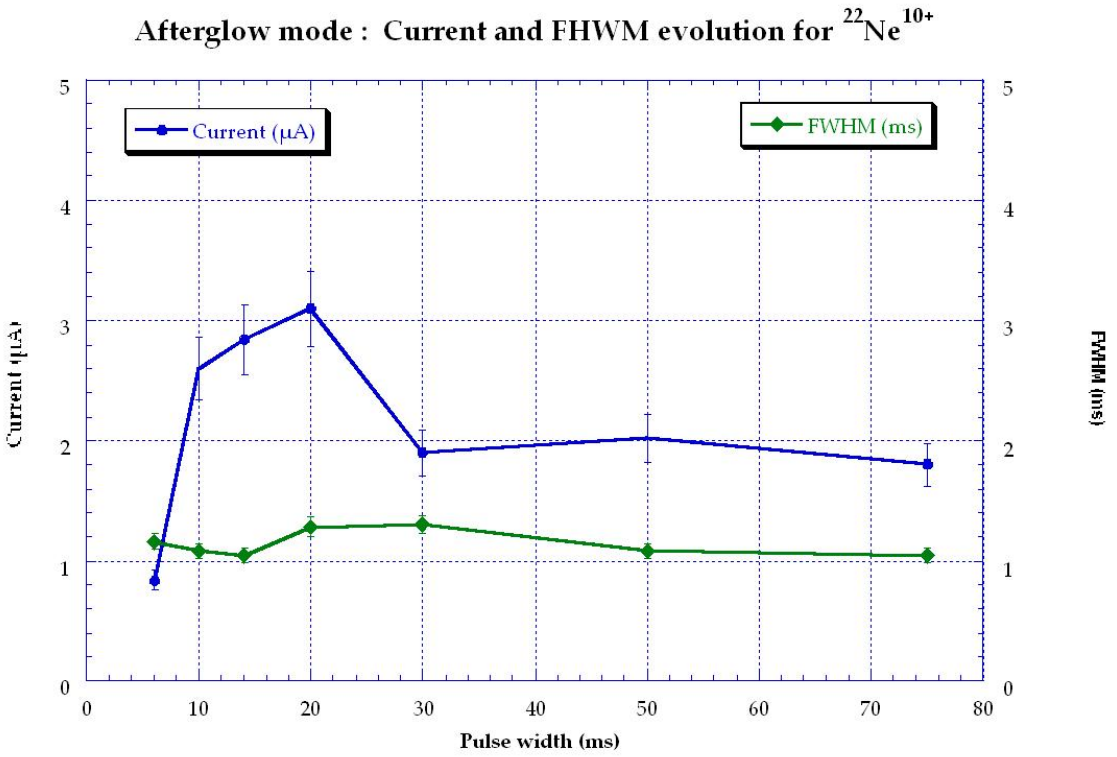

Figure 2

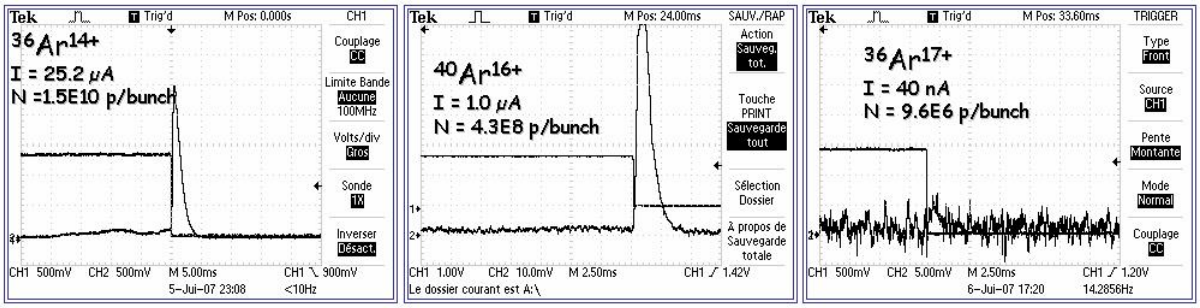

Figure 3

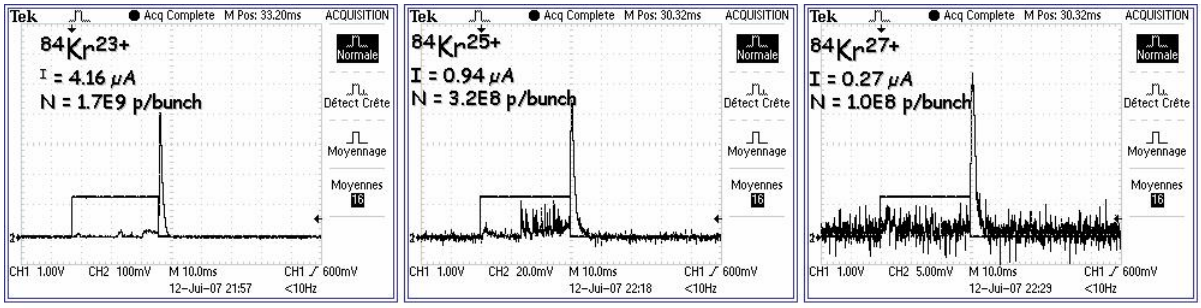

Figure 4

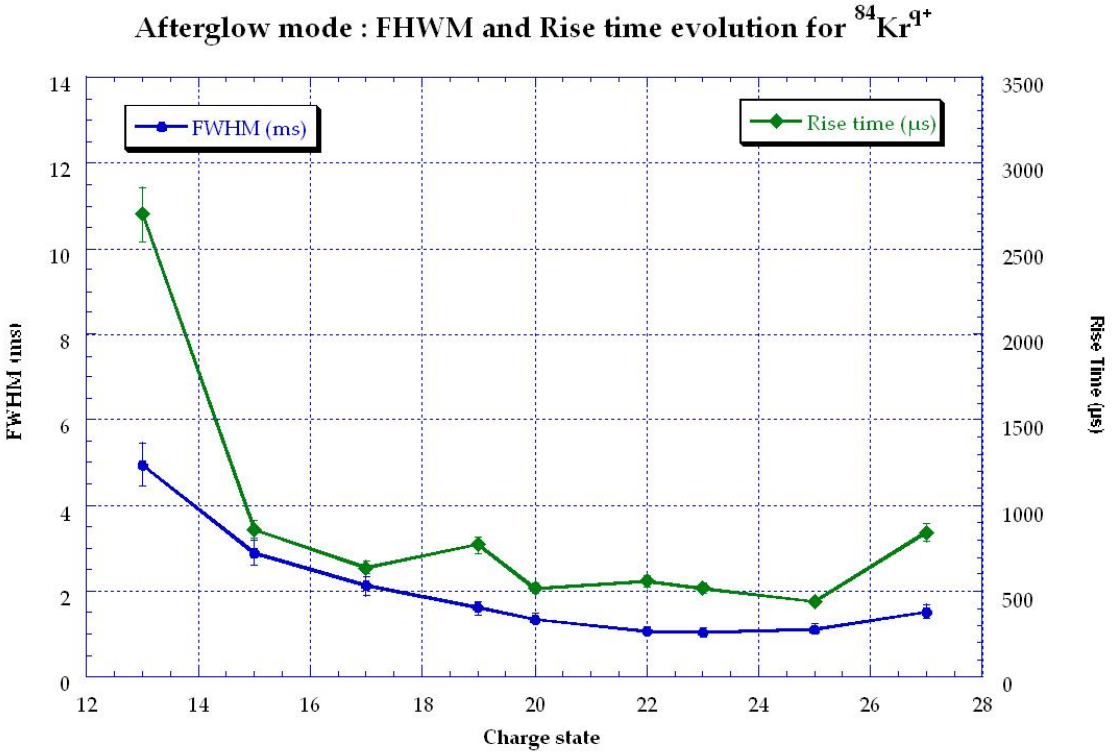

Figure 5

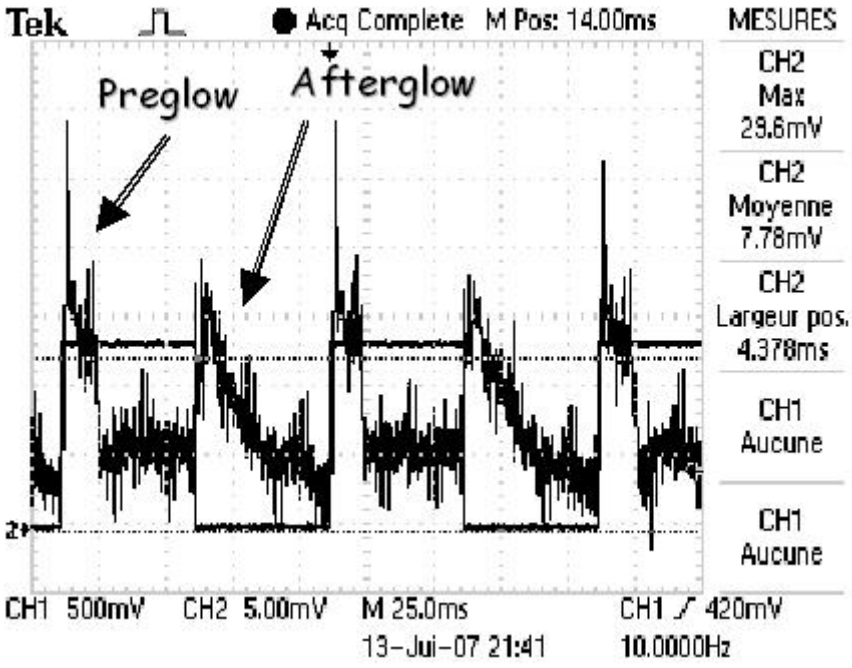

Figure 6

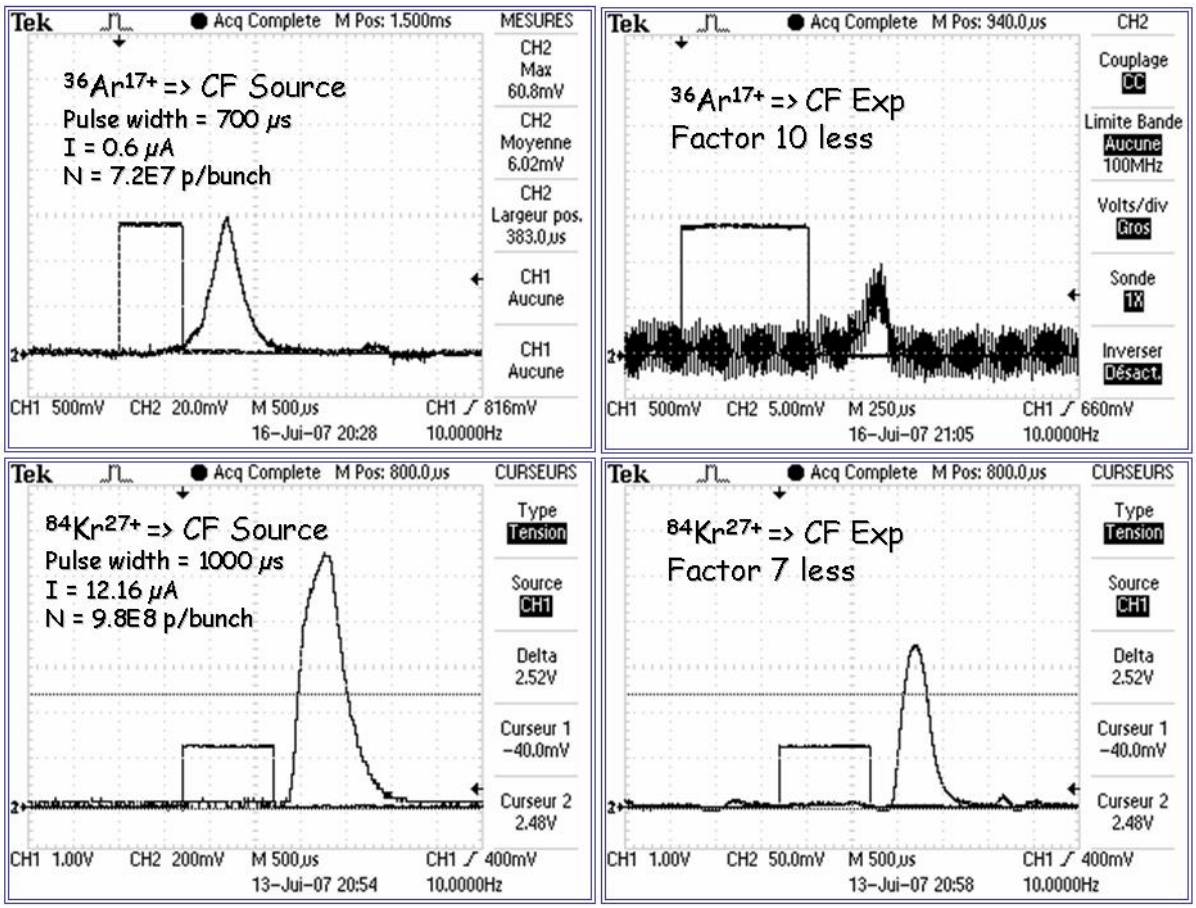

Figure 7

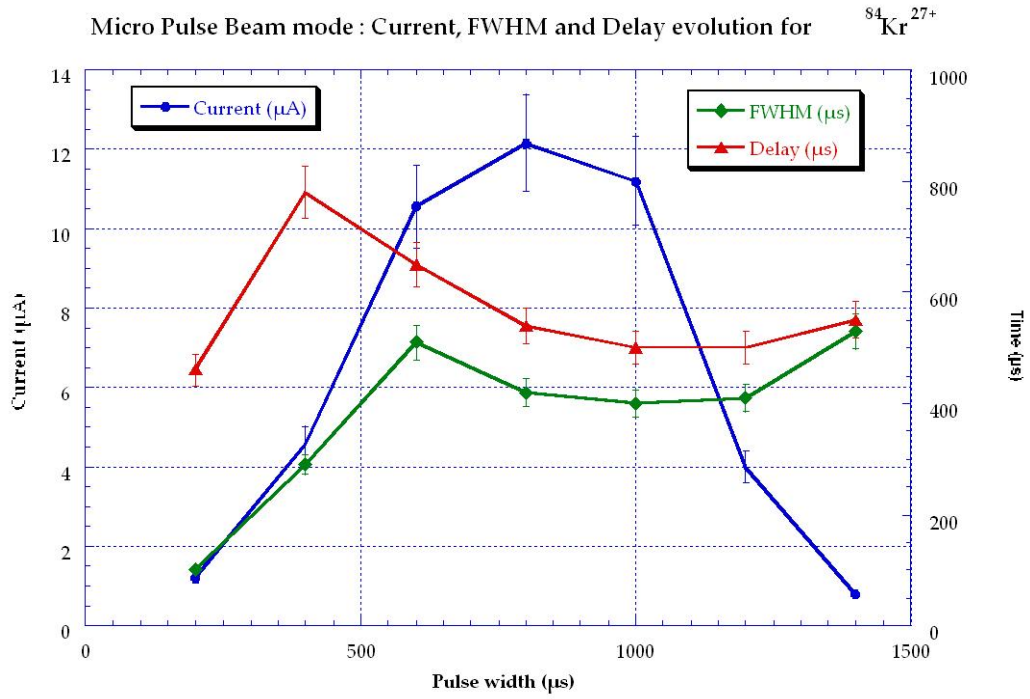

Figure 8

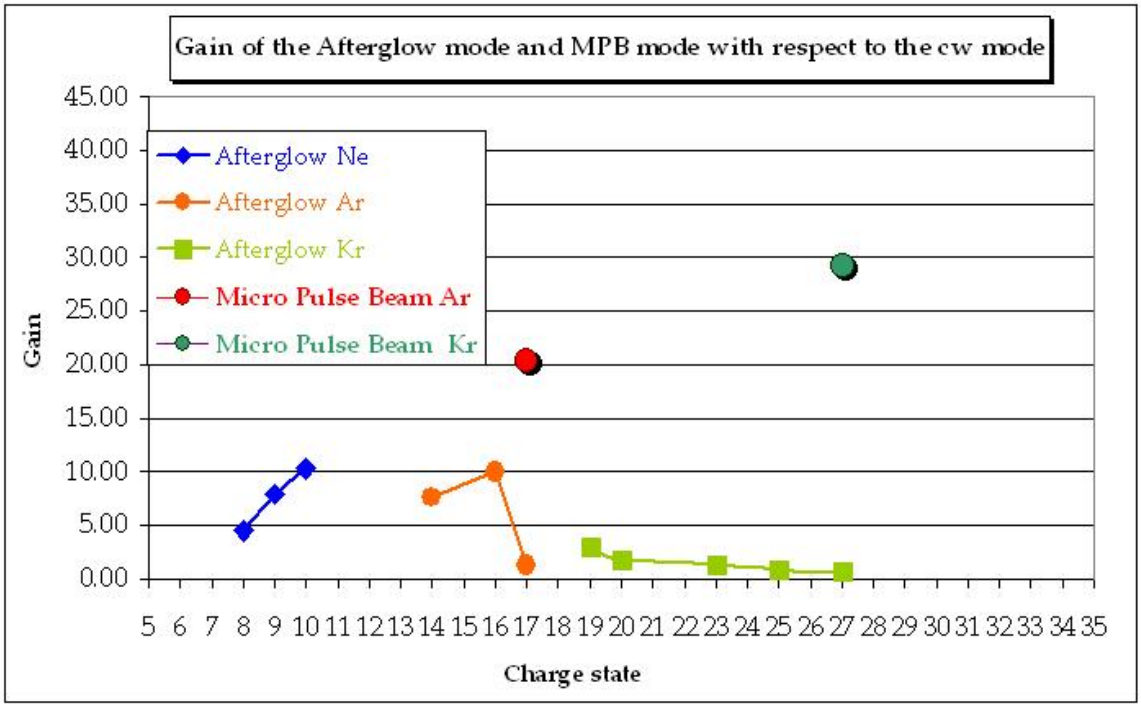

Figure 9

ATERGLOW MODE									
Element	**Q**	**I (A) CW mode**	**I (A) Afterglow mode**	**Pulse width (ms)**	**FWHM (ms)**	**Rise time (ms)**	**Fall time (ms)**	**Particles per bunch**	**Gain factor $I_{afterglow}/I_{CW}$**
Ne	8	55	252	14	1.03	0.61	4.83	2.95E+11	**4.58**
	9	4.3	33.8	14	1.36	0.63	3.02	2.90E+10	**7.86**
	10	0.4	4.1	14	1.04	0.42	1.54	2.80E+09	**10.25**
Ar	14	3.3	25.2	30	1.4	0.52	2.84	1.50E+10	**7.64**
	16	0.1	1	30	1.24	0.7	1.65	4.30E+08	**10.00**
	17	0.03	0.04	30				9.60E+06	**1.33**
Kr	19	11.5	33.6	30	1.61	0.77	2.83	1.82E+10	**2.92**
	20	7.7	13.6	30	1.36	0.52	2.52	6.67E+09	**1.77**
	23	3.2	4.16	30	1.04	0.52	1.84	1.70E+09	**1.30**
	25*	1.6	1.18	30	1.12	0.44	2.04	4.02E+08	**0.74**
	27*	0.52	0.34	30	1.52	0.84	1.2	1.26E+08	**0.66**

MPB MODE							
Element	**Q**	**I (A) CW mode**	**I (A) MPB mode**	**Pulse width (s)**	**FWHM (ms)**	**Particles per bunch**	**Gain factor I_{MPB}/I_{CW}**
Ar	17	0.03	0.6	700	0.34	7.20E+07	**20.33**
Kr	27*	0.52	12.1	1000	0.40	9.80E+08	**29.23**
	29*		0.07	400	0.4	3.60E+06	

*** These values are corrected depending on the horizontal slit width**

Table

Figure 1: Oscilloscope display of the afterglow peak for the $^{22}Ne^{9+ \text{ and } 10+}$

Figure 2: Evolution of the current and the FWHM of the afterglow peak versus the RF pulse width for $^{22}Ne^{10+}$ ions

Figure 3: Oscilloscope display of the afterglow peak for $^{36,40}Ar^{14+,\ 16+ \text{ and } 10+}$ ions

Figure 4: Oscilloscope display of the afterglow peak for $^{84}Kr^{23+,\ 25+ \text{ and } 27+}$ ions

Figure 5: Evolution of the FWHM of the afterglow peak and its rise time versus the charge state of the $^{84}Kr^{q+}$ ion

Figure 6: Oscilloscope display of the Preglow and the afterglow peaks for $^{84}Kr^{27+}$ ions

Figure 7: Oscilloscope display of the ion peak obtained in the MPB mode for $^{36}Ar^{17+}$ and $^{84}Kr^{27+}$ ions. The measurement has been done at the focal plane of the analysing dipole (left side) and at the end of the LHI-ARIBE beam line (right side).

Figure 8: Evolution of the FWHM of the ion peak obtained in the MPB mode for $^{84}Kr^{27+}$, its rise time and its delay versus the RF pulse width

Figure 9: Chart of the gain factor for the afterglow mode and the MPB mode

Table: Summary of the characteristics of the afterglow and MPB peaks for several ions